Application of the Method of Integral Relations to Real-Gas Flows Past Pointed Bodies

J. C. South Jr.* and P. A. Newman†
NASA Langley Research Center, Hampton, Va.

The method of integral relations is a numerical analysis technique that is suitable for solving the nonlinear partial differential equations of fluid mechanics. The present paper summarizes results obtained using the standard integral method as well as a modified method to calculate real-gas flow past pointed bodies. All results are compared with independent calculations by other methods. Specifically, the following flows have been computed: frozen flow past pointed bodies with arbitrary surface curvature; nonequilibrium flow past wedges and cones, vibrational relaxation in a pure diatomic gas or dissociation relaxation in the Lighthill-Freeman gas model. It is found that the approximate set of ordinary differential equations derived from the exact system of hyperbolic partial differential equations retains much of the character of the exact system. That is, the approximate set 1) forms an initial value problem where these values are determined from algebraic equations and 2) can be stably integrated only if the step size is controlled by a stability criterion related to the Mach line characteristic curves. It is concluded that the method of integral relations is generally applicable to supersonic flow past a pointed body and readily adaptable to machine calculation.

Nomenclature

a, b = nonequilibrium weighting functions [Eqs. (13)]
c_p = frozen-flow specific heat at constant pressure
C_p = surface pressure coefficient, $2(p_b - p_\infty)$
E = vibrational energy divided by $c_p T_\infty$
F, G, Q = see Eqs. (1)
k = number of independent exact partial differential equations
K = body curvature [Eqs. (2)]
M = frozen-flow Mach number
N = number of strips into which the shock layer has been divided
p = pressure divided by $\rho_\infty V_\infty^2$
s, n = coordinates along and normal to body surface, respectively
T = temperature divided by T_∞
u, v = velocity components in the s and n directions, respectively, divided by V_∞
V = total velocity divided by V_∞
x, r = coordinates along and normal to body axis, respectively
α = degree of dissociation, mass fraction of atoms
β = shock-wave inclination angle
δ = shock-layer thickness in the n direction
θ = body-surface inclination angle
ρ = density divided by ρ_∞

Subscripts

b = quantity evaluated on the body surface
c = corrected surface quantity
i = index [Eqs. (1)]
m = quantity evaluated on the midline of the shock layer
δ = quantity evaluated at the shock wave
∞ = quantity evaluated in the freestream

Introduction

SPECIFICALLY designed for high-speed computers, the method of integral relations is a numerical analysis technique for solving nonlinear partial differential equations. In applying the method to supersonic, inviscid-flow problems, one divides the shock layer into N strips for the Nth approximation. The governing partial differential equations, written in divergence form, are then integrated across these strips to obtain the approximating system of ordinary equations. For this integration certain integrands are replaced by Nth degree polynomials in the normal coordinate. The method and its applications in fluid mechanics have been reviewed recently by Belotserkovskii and Chushkin.[1] An obvious advantage of the method is that the highly efficient techniques for solving ordinary equations that have been developed for high-speed digital computers may be utilized. As in all integral methods the major disadvantage is lack of detail.

Most applications have been in mixed-flow problems such as the sonic flow past ellipses and ellipsoids and the supersonic flow past a blunt body. Other applications have treated conical flows without axial symmetry, nozzle flows, and the viscous boundary layer. Since these works considered ideal-gas flows, an obvious extension is the application of the method of integral relations to real-gas flows. Two such applications have been reported. Shih et al.[2] used the one-strip (i.e., first approximation) integral method to calculate nonequilibrium dissociating flow of a five-component (N_2, O_2, NO, N, and O) gas past a hemisphere; South[3,4] considered the flow of a vibrationally relaxing diatomic gas past wedges and cones using the first, second, and third approximations. Aside from the basic difference in the two problems (i.e., mixed elliptic-hyperbolic problem vs purely hyperbolic problem, respectively) there are differences in the manner in which the method has been applied to obtain the final approximating systems.

In applying the standard method to nonequilibrium flow past wedges and cones, South[4] found that the asymptotic value (far from the tip) of the surface vibrational energy did not converge as the order of the approximation increased. This is due to the improper weighting of the frozen-flow boundary condition at the shock wave. A modified procedure has been developed[5] which more properly weights this boundary condition as equilibrium is approached. The modification uses only one strip and replaces integrals by weighted averages of the integrands where the appropriate weighting is determined by considering the relaxation history along streamlines.

The purpose of the present paper is to summarize results obtained using the standard and modified integral methods to calculate real-gas flow past pointed bodies. Specifically, the following flows have been computed: 1) frozen or equi-

Presented as Preprint 65-27 at the AIAA 2nd Aerospace Sciences Meeting, New York, January 25–27, 1965; revision received May 14, 1965.

* Aerospace Engineer. Member AIAA.
† Aerospace Engineer.

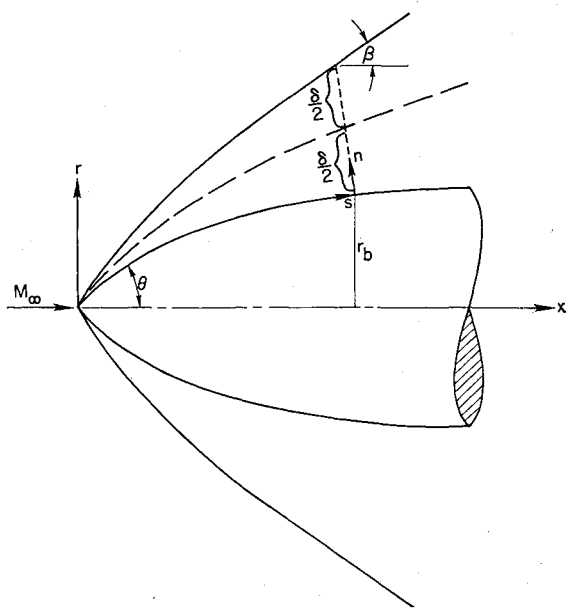

Fig. 1 Flow geometry, coordinate system, and strip arrangement for $N = 2$.

librium air flow past a circular cone at zero incidence ($N = 1$, 2); 2) frozen flow past pointed bodies with arbitrary surface curvature ($N = 2$); and 3) nonequilibrium flow: a) standard method, i.e., vibrational relaxation in a pure diatomic gas over a wedge ($N = 1, 2, 3$) and cone ($N = 1, 2$) or dissociation relaxation for the Lighthill-Freeman[6,7] gas over a wedge (N = 1), and b) modified method, i.e., vibrational relaxation in a pure diatomic gas over a wedge or dissociation relaxation for the Lighthill-Freeman gas over a wedge.

Results for the circular cone[4,8] are compared with those of Ref. 9 (frozen flow) and Romig[10] (equilibrium air). The vibrational relaxation results are compared with the characteristics results of Sedney et al.,[11,12] whereas the results for the Lighthill-Freeman "ideal dissociating gas" are compared with those of Capiaux and Washington.[13]

Problem Description

The physical problem discussed herein is the steady supersonic flow of a pure diatomic gas (or equilibrium mixture) past pointed bodies at zero incidence. The shock wave is attached at the tip and the flow is inviscid and isoenergetic. In nonequilibrium calculations for wedges and cones, only one dissipative mechanism is allowed to relax. Since several different gas models and body shapes are discussed herein, the reader is referred to Refs. 3–5 for explicit forms of the exact equations as well as the specific approximate equations that were used in the computations.

Exact Equations

The shock geometry and coordinate system for a pointed body of revolution are shown in Fig. 1 where the shock layer has been divided into two strips of equal width in the body-normal direction. The exact differential flow equations (continuity and both momentum equations), as well as the rate equation for a nonequilibrium calculation, are first written in a body-oriented, curvilinear s, n coordinate system.[14] Then each one is put into the divergence form, namely,

$$\partial Q_i/\partial s + \partial G_i/\partial n - F_i = 0 \qquad (i = 1 \text{ to } k) \qquad (1)$$

where the index i refers to a particular flow or rate equation. The functions Q_i, G_i, and F_i are known functions of s, n, and the k unknown dependent variables such as velocity components and pressure. For example, the continuity equation for the curved body shown in Fig. 1 is

$$(\partial/\partial s)(\rho u r) + (\partial/\partial n)[\rho v r(1 + Kn)] = 0 \qquad (2)$$

where $r = r_b + n\cos\theta$, and $K = -d\theta/ds$. The quantities Q_i, G_i, and F_i are easily identified. The number of dependent variables is reduced to the number k by using the equation of state and the total enthalpy equation.

Boundary Conditions

It is assumed that frozen flow exists across the shock wave. In a nonequilibrium calculation, then, the value of a nonequilibrium energy parameter does not change from its free-stream value as the fluid passes through the shock wave.

The location of the shock wave is computed from a differential equation that is determined from the geometry of the problem. For the body depicted in Fig. 1, this equation is

$$d\delta/ds = (1 + K\delta)\tan(\beta - \theta) \qquad (3)$$

The shock attachment condition requires that

$$\delta(0) = 0 \qquad (4)$$

Since the surface of the body is a streamline, the normal velocity component on the body must vanish for all values of s, that is,

$$v(s, 0) = v_b(s) = 0 \qquad (5)$$

Approximate Integral Solution

Standard Method

The method of integral relations provides a logical procedure for converting the exact Eq. (1) into an approximating system of ordinary equations. First, the shock layer is divided into a number of equal width strips. The accuracy of the approximation is improved by increasing the number of strips; however, for an arbitrary body, the algebra becomes very involved for more than two strips. Since it has been found that the two-strip approximation generally gives good results, this approximation has been depicted in Fig. 1 and the following remarks on the standard method will be for $N = 2$. Next, each of Eq. (1) is integrated over the body-normal coordinate n from the body surface to each of the strip boundaries. In this case then

$$\frac{d}{ds}\int_0^{\delta/2} Q_i dn - \frac{1}{2}Q_{i,m}\frac{d\delta}{ds} + G_{i,m} - G_{i,b} - \int_0^{\delta/2} F_i dn = 0 \qquad (6)$$

and

$$\frac{d}{ds}\int_0^{\delta} Q_i\, dn - Q_{i,\delta}\frac{d\delta}{ds} + G_{i,\delta} - G_{i,b} - \int_0^{\delta} F_i dn = 0 \qquad (7)$$

where $Q_{i,b}$ means Q_i evaluated on the body surface, subscript m refers to midline and subscript δ to shock wave. Leibnitz's rule for differentiation under the integral sign has been used in Eqs. (6) and (7).

The unknown integrals of (6) and (7) are evaluated by assuming second-order interpolation polynomials in n for the integrands Q_i and F_i; that is,

$$Q_i = q_{i,0} + q_{i,1}n + q_{i,2}n^2 \qquad (8)$$

where the coefficients $q_{i,0}$, etc., depend linearly on the functions $Q_{i,b}$, $Q_{i,m}$, and $Q_{i,\delta}$. The approximating set of $2k$ ordinary differential equations is obtained by substituting Eq. (8) into Eqs. (6) and (7). These equations are, respec-

tively,

$$2\delta \frac{d}{ds} Q_{i,m} + \delta \frac{d}{ds} Q_{i,\delta} + 4(Q_{i,m} - Q_{i,\delta}) \frac{d\delta}{ds} - G_{i,b} - 4G_{i,m} + 5G_{i,\delta} - \delta(2F_{i,m} + F_{i,\delta}) = 0 \quad (9)$$

$$\delta \frac{d}{ds} Q_{i,b} - \delta \frac{d}{ds} Q_{i,\delta} + (Q_{i,b} - 4Q_{i,m} + 3Q_{i,\delta}) \frac{d\delta}{ds} - 4(G_{i,b} - 2G_{i,m} + G_{i,\delta}) - \delta(F_{i,b} - F_{i,\delta}) = 0 \quad (10)$$

where $i = 1$ to k.

It should be noted that the quantities Q_i, G_i, and F_i contain geometric as well as the fluid and thermodynamic variables. We feel that it is more efficient, in terms of computational time, to algebraically obtain separate differential equations for $2k$ dependent variables and then numerically integrate the set, than to directly integrate Eqs. (9) and (10) (also $2k$ in number), and numerically separate the quantities of interest at each step. Thus considerable algebraic manipulation is required to obtain the computational set.

In previous ideal-gas studies, conservation of streamline entropy was used in lieu of the tangential-component momentum equation. In the nonequilibrium work of Shih et al.,[2] the rate and tangential-component momentum equations were included in the exact system, but were not integrated across the shock layer. These equations were applied in their exact forms along the surface, which is a streamline.

In our work, all of the partial differential equations, including the rate equation for a nonequilibrium flow, are integrated across the shock layer. Incongruities in the resulting approximating system occur; for example, the exact forms of the tangential-component momentum and rate equations were not satisfied at the surface. As the order of the approximation is increased, the numerical results indicate that these exact forms are more nearly satisfied.

Tip solution

The shock attachment boundary condition, Eq. (4), causes the coefficients of the derivatives in Eqs. (9) and (10) to vanish at the tip, since each contains the factor δ. [Note that $d\delta/ds$ is given by Eq. (3).] If a regular solution exists, then the remaining terms must also vanish at the tip. This condition leads to a system of nonlinear algebraic equations in $2k$ unknowns (after using the state and total enthalpy equations) which gives the tip solution. When a rate equation is included in the exact system, the result of applying the regularity condition to it is that the flow is frozen throughout the tip region.

Application of the preceding regularity condition has made the initial or tip derivatives indeterminate. These derivatives are evaluated by differentiating the approximate system and taking the limit as $s \to 0$. It is found that the initial derivatives so obtained are functions of the initial values. Thus the approximating system forms an initial value problem, where these initial values are obtained from limiting forms of the system at the tip.

Asymptotic rate equation

As previously stated, the rate equation is one of the members of the exact set for a nonequilibrium flow and is also converted to the ordinary differential equations (9) and (10). Far from the tip, $\delta \propto s$ so that $\delta \to \infty$ as $s \to \infty$. The frozen-flow boundary condition gives $dQ_{i,\delta}/ds = 0$, once the shock wave has attained its equilibrium inclination. Thus Eqs. (9) and (10) become, respectively,

$$(d/ds)Q_{i,m} = F_{i,m} + \tfrac{1}{2}F_{i,\delta} \quad \text{as} \quad s \to \infty \quad (11)$$

$$(d/ds)Q_{i,b} = F_{i,b} - F_{i,\delta} \quad \text{as} \quad s \to \infty \quad (12)$$

For a rate equation, Q_i contains the nonequilibrium energy parameter whereas F_i contains the driving force of the equation. Intuitively, the driving force should vanish throughout the shock layer when equilibrium is attained. The frozen-flow boundary condition, however, causes $F_{i,\delta}$ to be nonzero for all values of s. Thus it is seen from Eq. (12) that $(d/ds)Q_{i,b}$ does not vanish as it should due to the presence of $F_{i,\delta}$. It is seen that $F_{i,\delta}$ also appears in Eq. (11), but it receives less weight than $F_{i,m}$. For all approximations (any value of N), $F_{i,\delta}$ and $F_{i,b}$ appear in the surface rate equation and receive equal weight; only the sign between them changes with the order of the approximation. A modified procedure has been developed which more properly weights the relative contributions of $F_{i,\delta}$ and $F_{i,b}$ far downstream.

Modified Method

Polynomial profiles [Eq. (8)] are used in the standard method because they are expedient and can be logically extended to any desired approximation. For a nonequilibrium flow, however, the shock-layer profiles approach discontinuities far downstream due to the frozen-flow shock condition and cannot be adequately described by low-order polynomials. Although high-order polynomials would better describe these profiles, the algebra alone becomes prohibitive for more than three strips. The modification introduced in this section is an attempt to better account for these highly nonlinear profiles.

In the modified method only one strip is used and relative weighting of the quantities evaluated on the strip boundaries is adjusted to allow for nonequilibrium effects. The polynomial profiles assumed for certain integrands are not used. Integrals in Eq. (7) are replaced by

$$\int_0^\delta Q_i dn = \delta[(1 - a_i)Q_{i,b} + a_i Q_{i,\delta}]$$

$$\int_0^\delta F_i \, dn = \delta[(1 - b_i)F_{i,b} + b_i F_{i,\delta}] \quad (13)$$

where a_i and b_i, yet undetermined, are the nonequilibrium weighting functions for Q_i and F_i, respectively. Using Eqs. (13), Eq. (7) becomes

$$\delta(1 - a_i) \frac{d}{ds} Q_{i,b} + \delta a_i \frac{d}{ds} Q_{i,\delta} - \delta(Q_{i,b} - Q_{i,\delta}) \frac{da_i}{ds} + (1 - a_i)(Q_{i,b} - Q_{i,\delta}) \frac{d\delta}{ds} + G_{i,\delta} - G_{i,b} - \delta[(1 - b_i)F_{i,b} + b_i F_{i,\delta}] = 0 \quad (14)$$

where $i = 1$ to k. As in the standard method, Eqs. (14) must still be manipulated in order to obtain separate differential equations for k dependent variables. There are not enough independent conditions to determine all of the nonequilibrium weighting functions that have been introduced. Additional physical conditions must be used to determine the functions a_i and b_i.

For the modified wedge results presented herein, the weighting functions are determined independently as follows. With $\bar{Q}_i$ defined as

$$\bar{Q}_i = \frac{1}{\delta} \int_0^\delta Q_i \, dn \quad (15)$$

Eqs. (13) are solved for a_i (or b_i) giving

$$a_i = (\bar{Q}_i - Q_{i,b})/(Q_{i,\delta} - Q_{i,b}) \quad (16)$$

First, an approximate frozen-flow solution is used to obtain the shock geometry and streamline positions. Next, the streamline rate equation is integrated along the frozen-flow streamlines to determine the nonequilibrium variation of Q_i. Then Q_i is integrated across the shock layer to get

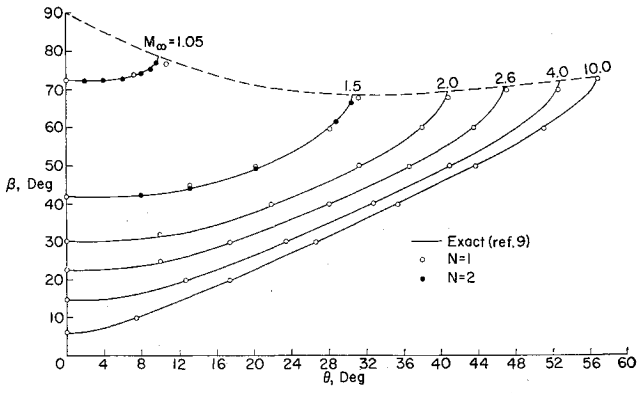

Fig. 2 Shock-wave inclination vs cone semivertex angle for frozen flow.

$\bar{Q}_i$, defined by Eq. (15). Finally a_i, a function of s, is computed from Eq. (16).

For a wedge, the frozen-flow shock wave and streamlines are straight. Reference 11 shows that little error is introduced if the velocity is held constant while the streamline rate equation is integrated. These two approximations allow one to reduce the determination of the weighting functions to a single integration over s, which can be performed along with the integration of the approximating set, Eqs. (14). For more complex flows, these simplifying approximations are not valid and the determination of the weighting functions will not be so easy.

Tip solution

Just as in the standard method, the shock attachment condition causes the coefficients of the derivatives in Eqs. (14) to vanish at the tip. Again the regularity condition requires the remaining terms to vanish and leads to a system of nonlinear algebraic equations, in k unknowns. However, the weighting functions must be determined independently. The initial derivatives are again found to be functions of the initial values. For a wedge, the initial value of all the weighting functions is $\frac{1}{2}$, so that the modified and one-strip standard solutions are the same in the tip region.

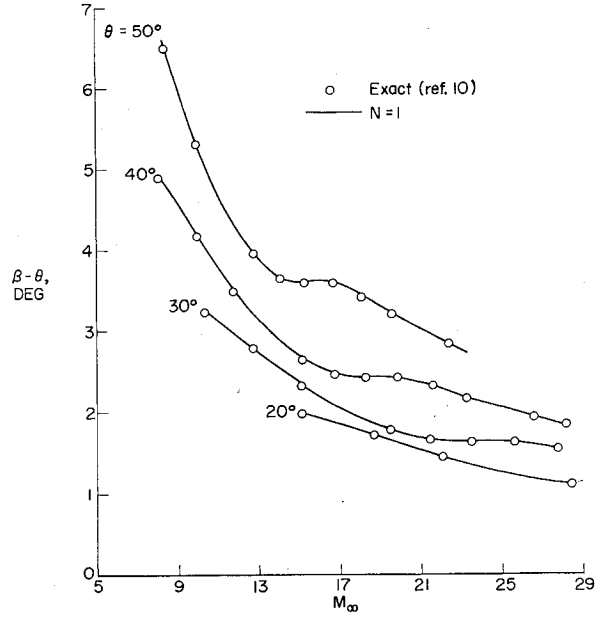

Fig. 3 Angular shock-layer thickness vs freestream Mach number for equilibrium flow of air past a cone; $p_\infty = 10^{-3}$ atm and $T_\infty = 273°$K.

Asymptotic behavior

Far from the tip, most of the shock layer is in equilibrium so that the weighting functions are changing very little with s. Thus,

$$da_i/ds \to 0 \qquad \text{as} \qquad s \to \infty \tag{17}$$

Furthermore, since $Q_{i,\delta} \neq Q_{i,b}$ and $\bar{Q}_i \to Q_{i,b}$ as $s \to \infty$, Eq. (16) gives

$$a_i \to 0 \qquad \text{and} \qquad b_i \to 0 \qquad \text{as} \qquad s \to \infty \tag{18}$$

As stated when discussing the standard method, $\delta \to \infty$ as $s \to \infty$ and, for a rate equation, $(d/ds)Q_{i,\delta} \to 0$ as $s \to \infty$. Thus application of Eqs. (17) and (18) and the preceding to Eqs. (14) gives

$$(d/ds)Q_{i,b} = F_{i,b} \qquad \text{as} \qquad s \to \infty \tag{19}$$

Equation (19) does not contain $F_{i,\delta}$, the term that caused the asymptotic form of the rate equation of the standard method [Eq. (12)] to give the improper surface energy asymptote.

Since the rate equation of the modified method has the proper asymptotic form, an algebraic asymptotic solution can be obtained. The driving force of the rate equation (a factor in $F_{i,b}$) vanishes when equilibrium is reached so that the rate equation can be replaced by the equilibrium condition. The requirement that the other derivatives vanish coupled with Eqs. (17) and (18) gives the algebraic asymptotic solution. For a wedge, this solution gives the same shock-wave inclination and body-surface properties as the equilibrium-flow solution. However, the properties immediately behind the shock wave have the frozen-flow values, not the equilibrium-flow values.

Numerical Results

For frozen or equilibrium flow past a cone (body curvature zero) similarity considerations show that the shock wave is straight and flow properties remain constant along rays emanating from the tip. In this case every strip boundary is a ray, and thus the s derivatives of the physical variables must vanish for all values of s. Applying this condition to the approximating set yields the same algebraic solution for all s as that previously obtained for the tip solution.

Tip Solution

Figure 2 illustrates the agreement of the shock-wave inclination computed from the approximate[4] conical solution with that from the exact[9] numerical solution for frozen flow.

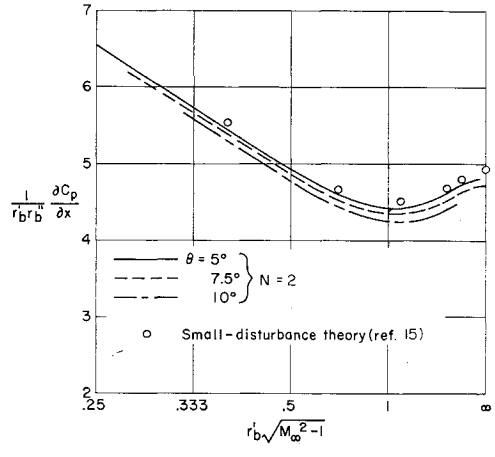

Fig. 4 Surface pressure-coefficient gradient vs a combined supersonic-hypersonic similarity parameter at the ogive tip.

The abscissa is the cone semivertex angle θ. Results for both the first and second approximations are shown where they differ. It can be seen that the second approximation is better for $M_\infty < 2$, but that both agree very well for $M_\infty > 2$. Figure 3 shows the angular shock-layer thickness $\beta - \theta$ (vs M_∞) as computed from the first approximation[8] for air in thermodynamic equilibrium. The agreement with the exact numerical solution computed by Romig[10] is seen to be good, the average difference being about 1%.

Initial values for a pointed body with arbitrary surface curvature are the same as those for a body with no curvature; the initial derivatives, however, are nonzero due to the curvature terms. Figure 4 shows the gradient of the surface pressure coefficient at the ogive tip in the form suggested by Van Dyke's[15] hypersonic small disturbance theory. The abscissa is the combined supersonic-hypersonic similarity parameter. As the semivertex angle is decreased, the present results appear to converge on those of the small disturbance theory, which is exact in the limit $\theta \to 0$.

Hypersonic Stability Criterion

In attempting to integrate some cases away from the tip, it was found that a stability criterion related to the Mach line characteristics had to be applied. For simplicity, we show in Fig. 5 a straight body where the shock layer is divided into two strips. Data are known at the shock wave, on the midline, and on the surface (denoted by the circles in Fig. 5). The maximum integration step size Δs which can be used is determined from the intersection of the characteristics. An approximate criterion on Δs is obtained by assuming that the streamlines are parallel to the surface and the local Mach number is equal to the surface Mach number M_b. For two strips this criterion is

$$\Delta s \leqq (\delta/4)(M_b^2 - 1)^{1/2} \tag{20}$$

The effect of applying the criterion of Eq. (20) is shown in Fig. 6. Note that in this case, the solution with the fixed step size quickly became stable once that step size satisfied the stability criterion. This criterion must be applied in both the standard and modified methods. The approximate

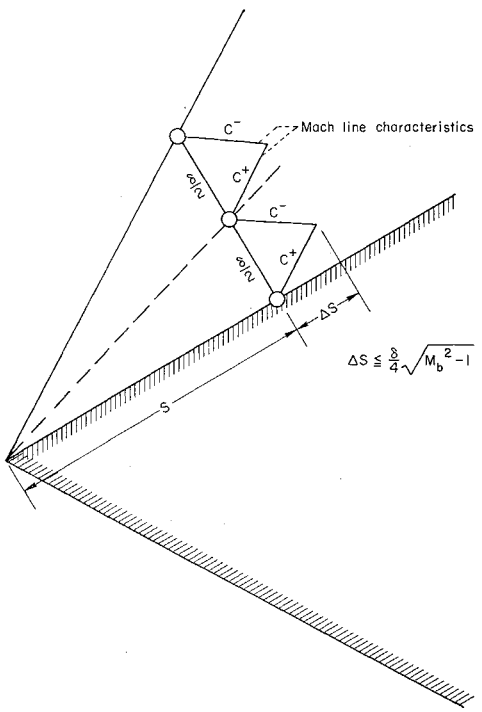

Fig. 5 Approximate hyperbolic stability criterion for $N = 2$.

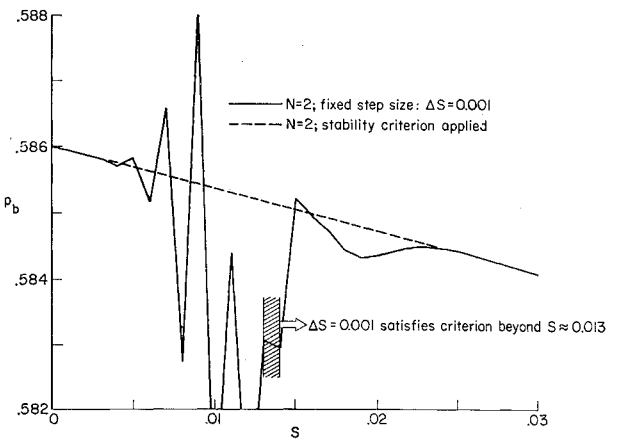

Fig. 6 Effect of hyperbolic stability criterion on surface pressure.

system thus appears to retain the character of the original hyperbolic system.

Frozen Flow

Xerikos and Anderson[16] have questioned the applicability of the method of integral relations in the supersonic flow regime for good reason: the influence of the surface boundary propagates along the normal coordinate rather than along the left-running (C^+) characteristic. We find that even though this is true, the method partially compensates for this anomalous behavior. Details concerning this point are given in Ref. 17.

Figure 7 shows the variation of the surface pressure coefficient with x (the axial distance, nondimensionalized by the afterbody diameter) for frozen flow past a three-segment, pointed axisymmetric body. It is seen that the agreement with characteristics is good. For some cases with larger semivertex angles and middle-segment curvatures, the surface pressure becomes negative near the shoulder and the integration stops.[17] For these cases, there are strong entropy gradients in the shoulder region and apparently the two-strip approximation is not accurate enough to adequately account for them.

Nonequilibrium Flow

In order to compare the standard and modified integral results with one another as well as with existing characteristics computations, the nonequilibrium results are divided according to gas models. These results are restricted to flow over wedges and cones for the standard method and wedges only for the modified method. Details such as the

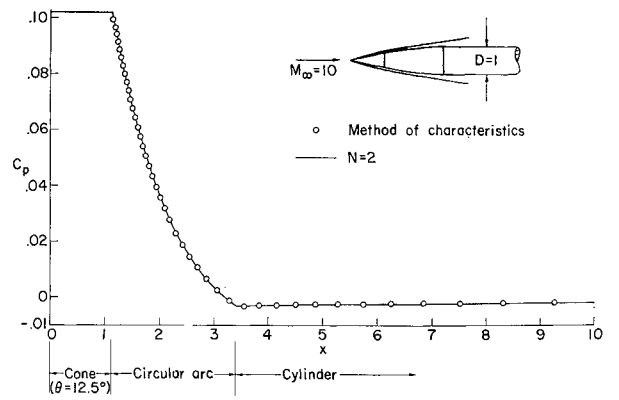

Fig. 7 Surface pressure coefficient vs axial distance for frozen flow past a cone, circular arc, cylinder; $\theta = 12.5°$ and $M_\infty = 10$.

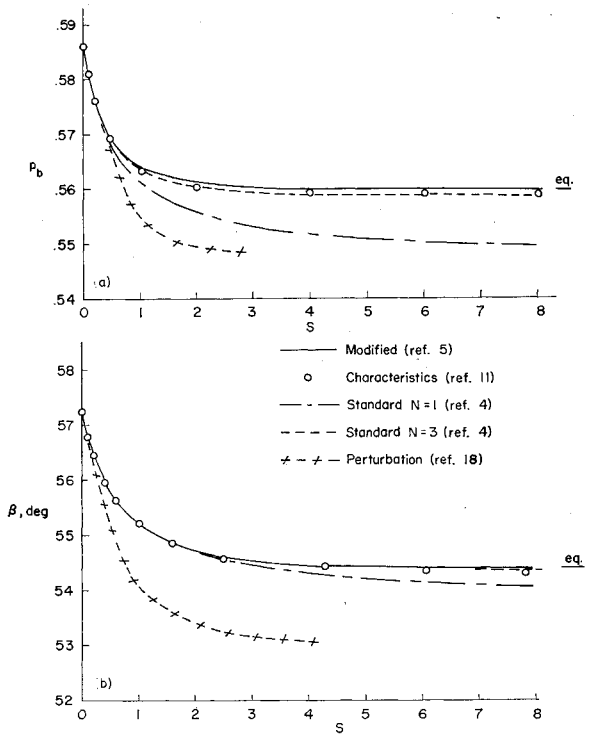

Fig. 8 Surface pressure and shock-wave inclination vs nondimensional surface distance for a wedge: case I.

characteristic temperatures, nonequilibrium rate parameters, rate equations, and length scales (which are used to nondimensionalize the distances) are given in Ref. 3–5.

Vibrational relaxation

Two cases, a wedge and a cone, are considered for vibrational relaxation. In both, the gas is pure nitrogen and the freestream temperature is taken as 300°K. The following conditions apply: in case I, wedge: $M_\infty = 6$ and $\theta = 40.02°$, and in case II, cone: $M_\infty = 12$ and $\theta = 46.39°$. The characteristics results for case I are given in Ref. 11 and those for case II in Ref. 12.

The results for the surface pressure and shock-wave inclination for case I are shown as a function of nondimensional surface distance in Fig. 8. Standard integral results for $N = 1$ and $N = 3$, modified integral results, characteristics results, and recent perturbation[18] results are given. Standard integral results for $N = 2$ lie very close to those for $N = 3$, and so are omitted in order to avoid confusion in the figure. The tick marks labeled "eq." are the appropriate equilibrium-flow values that both the pressure and shock angle should have as asymptotes. It is seen that the modified method gives better asymptotes than the standard method and that the three-strip standard results are better than the one-strip results.

The surface pressure distribution and shock angle for case II are shown in Fig. 9. Standard integral results for $N = 1$ and $N = 2$ and characteristics results are given. The detrimental effect of the improper surface rate equation on the surface pressure can be seen in Fig. 9a. The $N = 2$ results are much better than those for $N = 1$, and it is felt that for both of these cases, the approach to equilibrium is adequately described by two strips.

As mentioned previously, the tangential momentum and rate equations of the approximating set are not equivalent to the exact momentum and rate equations along the surface. This is due to the fact that the exact equations have been integrated across the shock layer and must necessarily account for properties within the shock layer. The exact surface momentum and rate equations are integrated in addition to the approximating set in order to obtain corrected values of the remaining surface variables. It is tempting to replace the two corresponding equations of the approximating system with these two exact equations, but South[4] finds that such a "hybrid" system is unstable. If only the exact rate equation is used in lieu of its approximate counterpart, the asymptotes are worse than those of the complete approximating system. Such a "hybrid" system was used in the nonequilibrium blunt-body study of Shih et al.[2]

In Fig. 10, the surface vibrational energy and temperature from the approximating system as well as those from corrected equations for case I are compared with the characteristics results. This figure shows the nonconvergence of the vibrational energy due to the improper rate equation of the standard method. The modified results go asymptotically to the equilibrium-flow values (tick marks labeled "eq."). Curves labeled C are the corrected results for both integral methods (all approximations) to the scale of the figure. These corrected equations must be integrated in order to obtain the surface entropy-layer effects. The manner in which the upper limit to these effects is computed is not known. It appears that for the cases considered, the equilibrium condition for the frozen-flow shock-wave inclination gives values that are upper bounds for the corrected asymptotes. (This corresponds to the equilibrium-flow solution for a body with a larger vertex angle.) The tick marks labeled "fr." give these values.

Dissociation relaxation

The dissociation relaxation case considered is for flow of the Lighthill-Freeman "ideal dissociating gas" past a wedge. The parameters for this case, called case III herein, correspond to oxygen where the freestream conditions are about those for an altitude of 150,000 ft. For case III (wedge) the following conditions apply: $M_\infty = 32$ and $\theta = 25.175°$. The characteristics results for this case are presented as case I in Ref. 13.

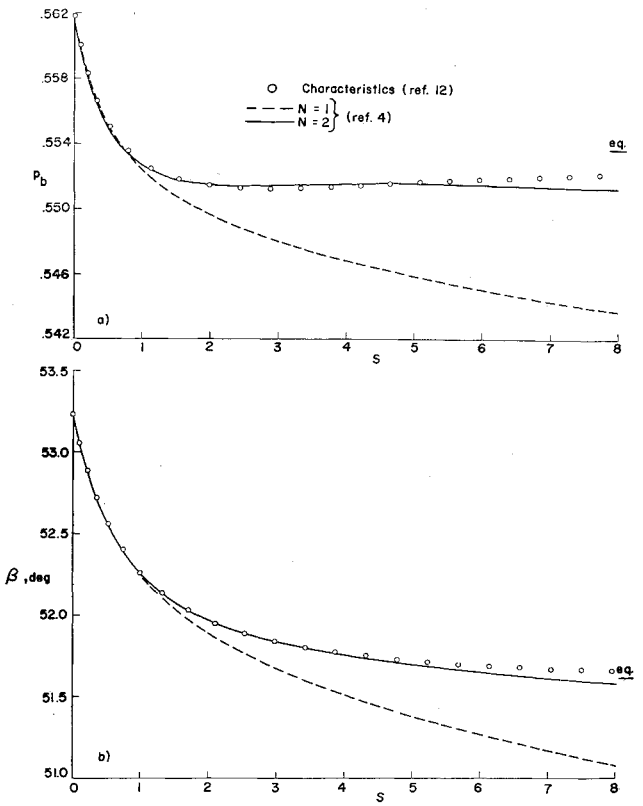

Fig. 9 Surface pressure and shock-wave inclination vs nondimensional surface distance for a cone: case II.

Results for the surface pressure and shock-wave inclination are presented in Fig. 11 as a function of the nondimensional surface distance. It appears that the highly nonlinear shock-layer profiles cause the one-strip standard results to depart significantly from the characteristics results. The modified results have been computed using weighting functions determined from both the frozen-flow and equilibrium-flow shock inclinations and streamline geometries. Again, the tick marks labeled eq. are the equilibrium-flow values.

The surface degree of dissociation and corrected temperature are plotted in Fig. 12. The corrected equations must be used in order to obtain the surface entropy-layer effects. Figure 12 shows that the corrected quantities from both integral methods are indistinguishable when plotted to the scale chosen. The tick marks labeled "fr." are the equilibrium-flow values for the frozen-flow shock-wave inclination. It is seen that the corrected integral method asymptotic values are bounded by the tick marks, but that the characteristics results for the surface temperature asymptote does not appear to fall between the tick marks. Characteristics results of case I for both the surface vibrational energy and surface temperature did asymptotically fall between the "fr." and "eq." tick marks.

Conclusions

The numerical results indicate that the method of integral relations can be used to obtain good shock-wave shapes and pressure distributions. The success of the modified integral method for more complex flows should not be inferred from the modified results presented herein, since these results have been obtained only for wedge flow, a very simple flow. Several general features have been observed concerning the application of the method of integral relations to supersonic real-gas flows over pointed bodies.

1) The approximating system forms an initial value problem; this would be the correct problem for the exact system of hyperbolic partial differential equations. The initial values are determined from algebraic equations that are the limiting forms of the approximating system at the body tip.

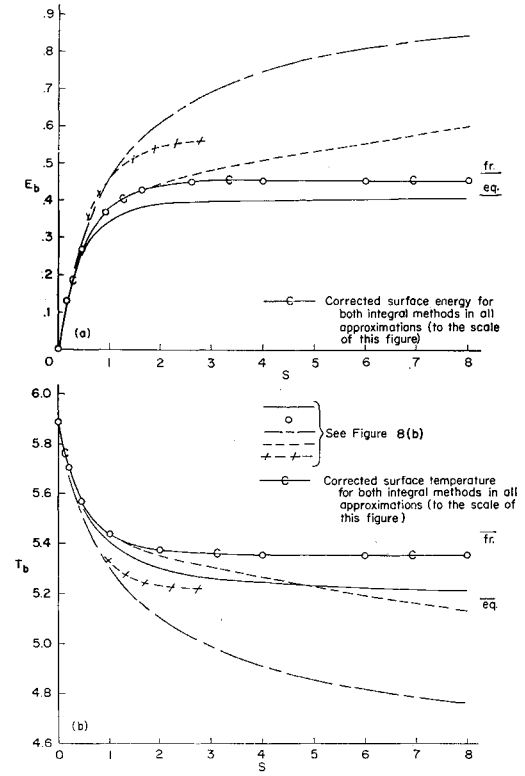

Fig. 10 Surface vibrational energy and temperature vs nondimensional surface distance for a wedge: case I.

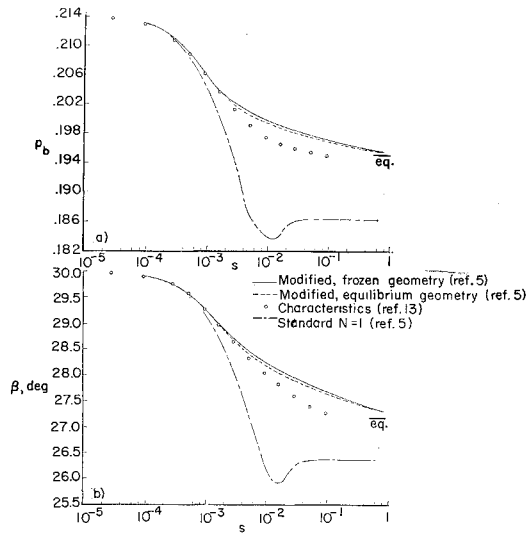

Fig. 11 Surface pressure and shock-wave inclination vs nondimensional surface distance for a wedge: case III.

2) An approximate algebraic solution, valid for frozen or equilibrium conical flow, is obtained from the approximating system as a special case. This solution is the same as that for the nonequilibrium initial values mentioned previously.

3) A stable integration of the approximating system of ordinary differential equations is obtained only if the integration step size is controlled by a stability criterion related to the Mach line characteristic curves. Thus, the approximating system appears to retain much of the character of the original hyperbolic equations.

4) Even though the surface boundary signals propagate along the body-normal direction instead of the left-running characteristic curve, the integral method partially compensates for this anomalous behavior.

5) The exact forms of the surface rate and tangential-component momentum equations cannot be used successfully in lieu of their counterparts in the approximating system. However, they are used as auxiliary equations to yield improved distributions for the surface quantities such as temperature, density, and velocity.

6) For nonequilibrium flow past wedges and cones, the two-strip standard method of integral relations gives good over-all results. Although the approximate rate equation

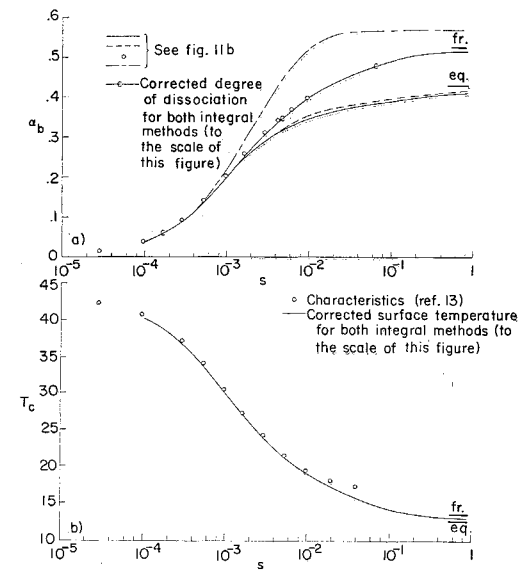

Fig. 12 Surface degree of dissociation and temperature vs nondimensional surface distance for a wedge: case III.

does not exhibit correct asymptotic behavior in any approximation, the affected variables can be corrected as indicated in 5.

7) The modified method gives better asymptotic results than does the standard method for nonequilibrium flow past a wedge. It is still necessary to apply the corrections noted in 5 to obtain the surface entropy-layer effects.

It is concluded that the method of integral relations is generally applicable to supersonic real-gas flow past pointed bodies. Furthermore, the method is simple in formulation and readily adaptable to machine calculation.

References

[1] Belotserkovskii, O. M. and Chushkin, P. I., "The numerical method of integral relations," Zh. Vychislitel'noy Mat. Mat. Fiz. II, 731–759 (1962); also NASA TTF 8356 (January 1963).

[2] Shih, W. C. L., Baron, J. R., Krupp, R. S., and Towle, W. J., "Nonequilibrium blunt body flow using the method of integral relations," TR 66, Contract NOw 62-0765-d, Aerophysics Lab., Massachusetts Institute of Technology (May 1963).

[3] South, J. C., Jr., "Application of Dorodnitsyn's integral method to nonequilibrium flows over pointed bodies," NASA TN D-1942 (1963).

[4] South, J. C., Jr., "Application of the method of integral relations to supersonic nonequilibrium flow past wedges and cones," NASA TR R-205 (1964).

[5] Newman, P. A., "A modified method of integral relations for supersonic nonequilibrium flow over a wedge," NASA TN D-2654 (1965).

[6] Lightbill, M. J., "Dynamics of a dissociating gas—Part I. Equilibrium flow," J. Fluid Mech. **2**, 1–32 (1957).

[7] Freeman, N. C., "Dynamics of a dissociating gas—Part III. Nonequilibrium theory," AGARD Rept. 133, North Atlantic Treaty Organization (Paris) (July 1957).

[8] Newman, P. A., "Approximate calculation of hypersonic conical flow parameters for air in thermodynamic equilibrium," NASA TN D-2058 (1964).

[9] "Equations, tables, and charts for compressible flow," NACA Rept. 1135 (1953).

[10] Romig, M. F., "Conical flow parameters for air in dissociation equilibrium," Research Rept. 7, Convair Science Research Lab. (May 1960).

[11] Sedney, R., South, J. C., and Gerber, N., "Characteristic calculation of nonequilibrium flows," Rept. 1173, Ballistic Research Labs., Aberdeen Proving Ground (April 1962).

[12] Sedney, R. and Gerber, N., "Nonequilibrium flow over a cone," Rept. 1203, Ballistic Research Labs., Aberdeen Proving Ground (May 1963).

[13] Capiaux, R. and Washington, M., "Nonequilibrium flow past a wedge," AIAA J. **1**, 650–660 (1963).

[14] Hayes, W. D. and Probstein, R. F., *Hypersonic Flow Theory* (Academic Press, Inc., New York, 1959), Chap. V, pp. 163–173.

[15] Van Dyke, M. D., "A study of hypersonic small-disturbance theory," NACA Rept. 1194 (1954).

[16] Xerikos, J. and Anderson, W. A., "A critical study of the direct blunt body integral method," Douglas Rept. SM-42603, Douglas Aircraft Co. (December 1962).

[17] South, J. C., Jr. and Newman, P. A., "Supersonic flow past pointed bodies," AIAA J. **3**, 1019–1021 (1965).

[18] Lee, R. S., "A unified analysis of supersonic nonequilibrium flow over a wedge: I Vibrational nonequilibrium," AIAA J. **2**, 637–646 (1964).